Proceedings of the 4th International Conference on Multiphase Flow (ICMF), New Orleans, LA (USA), May 27-June 1, 2001, Ed. E. E. Michaelides(CD-ROM), paper 937, Tulane University (2001).

CHF as a Non-Equilibrium Drying Transition

V. S. Nikolayev*, D. A. Beysens*,
ESEME, Service des Basses Temperatures, CEA Grenoble,
17, rue des Martyrs, 38054, Grenoble Cedex 9, France,
Y.Garrabos,
ESEME-CNRS,
Institut de Chimie de la Matière Condensée de Bordeaux,
87, Av. du Dr. Schweitzer, 33608 Pessac Cedex, France
and J. Hegseth
Department of Physics, University of New Orleans,
New Orleans, LA 70148, USA

July 15, 2001

Abstract

The Critical Heat Flux (CHF) phenomenon is the formation of a vapor film between the heater and the liquid when the heat supply exceeds a critical value, the critical heat flux value. We propose a physical explanation for the CHF that is based on the spreading of the dry spot under a vapor bubble. The spreading is initiated by the vapor recoil force, a force coming from the uncompensated mechanical momentum of the fluid molecules being evaporated into the bubble. Since the evaporation intensity increases sharply near the triple (gas-liquid-solid) contact line, the influence of the vapor recoil can be interpreted in terms of an increase of the apparent contact angle. As the vapor recoil force is always directed towards the liquid side, it increases the dry spot under the bubble. Therefore, for the usual case of complete wetting of the heating surface by the liquid, the CHF can be understood as an out of equilibrium drying transition from complete to partial wetting. The value of the CHF should be close to that defined by the equality of the contributions of the vapor recoil and the surface tension. We present the results of a 2D numerical simulation of the bubble growth at high system pressure when the bubble is assumed to grow slowly, its shape being defined by the surface tension and the vapor recoil force. The numerical results confirm this physical mechanism of the boiling crisis.

Near the gas-liquid critical point of a given fluid, the bubble growth is very slow. The increase of the apparent contact angle was observed experimentally together with the growth of the dry spot, thus confirming the proposed explanation.

Key words: Boiling, bubble growth, CHF, contact angle, recoil force

*Mailing address: ESEME-CEA, Institut de Chimie de la Matière Condensée de Bordeaux, 87, Av. du Dr. Schweitzer, 33608 Pessac Cedex, France

1 Introduction

When the heat flux from the heater exceeds a critical value (the Critical Heat Flux, CHF) during boiling, the vapor bubbles on the heating surface abruptly form a film that thermally insulates the heater from the liquid. In other words, the heater dries out. The heat transfer is blocked and the temperature of the heater rapidly grows. This phenomenon is known under the names of "boiling crisis," "burnout," or "departure from nucleate boiling" (Tong 1997). Because the boiling crisis is very rapid under usual conditions, the correct CHF estimation requires a clear understanding of the physical phenomenon that triggers it. Numerous models were proposed, so that completely different mechanisms are assumed to be responsible for the different regimes of boiling (pool or flow boiling, bubble or slug regimes of flow, degree of underheating of the bulk fluid, different system pressures or heater geometries, etc.). The underlying hypotheses for these models are either controversial or unjustified at all. An excellent discussion and classification of the existing CHF models can be found in the recent works (Brusstar *et al.* 1998, Buyevich 1999). This situation is closely related to the experimental difficulties with the observations of the boiling crisis. For reasons of industrial importance, the most common boiling experiments are carried out in Earth gravity at low (atmospheric) system pressures as compared to the critical pressure of the given fluid. The CHF value is large for these low pressures. The violence of boiling at large heat fluxes makes observations very difficult. However, several important features of the boiling crisis that can help to understand the underlying physics have nevertheless been firmly established. The most important among them is the *local* nature of boiling crisis. It begins in a thin layer of liquid adjacent to the heating surface and at a definite spot. In most cases of flow boiling this layer can be assumed quiescent because of the no-slip boundary condition for the fluid velocity at the heating surface. Therefore, we believe it is unnecessary to assume different physical causes for the boiling crisis according to the different conditions or regimes of boiling, and that the crisis should be induced by the *same physical phenomenon* (Bricard *et al.* 1997) in most cases. The occurrence of the boiling crisis is influenced by the values of only a few parameters of this thin layer, the most important being the wetting conditions (Diesselhorst *et al.* 1981) and the distribution of temperature. The exact value of the CHF thus depend on the particular conditions of boiling through these parameters.

There are two possible scenarios for the beginning of the heater drying. Either the dry spot under a vapor bubble begins to grow independently of other bubbles or many neighboring bubbles begin to coalesce thus creating a growing dry spot. The second option was analyzed carefully by Bricard *et al.* (1997). It has been shown that this scenario requires repetitive (at least 30 – 40 times) formation of aggregates of 2 – 3 coalesced bubbles at the same nucleation spot. This is not a likely event because in order to coalesce, 1) the bubbles should grow close to each other, which is not a likely event itself (Kenning and Del Valle (1981), Pasamehmetoglu and Nelson (1991)), and 2) their interfaces should be pushed in to each other to overcome the strong lubrication forces between them (Yiantsios and Davis 1991) by some force which is difficult to identify. A fact of primary importance for the boiling crisis was established by van Ouwerkerk (1972) and Torikai *et al.* (1991) who show that the boiling crisis appears as a result of the fast growth of a dry spot under a *single* bubble.

Another important step was the revelation of the strong influence of the bubble residence time (or bubble departure time, the time between bubble nucleation and bubble

departure from the heating surface) t_{dep} on the CHF (Brusstar *et al.* 1999). The residence time depends on the value of lift-off forces that tend to remove the bubble from the heater. These forces can be varied, e.g., by inclining the heating surface or by conducting the boiling experiment on board of a spacecraft (Brusstar and Merte 1998). A strong decrease of the CHF with the increase of t_{dep} was shown. The long residence time allows the bubble growth to be observed in more detail. However, these low pressure observations remain difficult because the bubble growth rate is as large as in conventional experiments. The resulting violent liquid motion still hinders the observations of the heater dry-out. In section 4 we discuss the results of our experiment (Garrabos *et al.* 1999) carried out in microgravity environment (Mir space station) with a fluid at high pressure close to its critical point, where the CHF is very small and the bubble growth is very slow when the heat supply approaches the CHF.

The importance of the dry spot growth was recognized in a large number of the CHF models (see Bricard *et al.* (1997) for a review) that are based on a concept of a microlayer dryout. The microlayer model (Cooper and Lloyd 1969) postulates the existence of a thin liquid film (microlayer) between the heater and the foot of the vapor bubble. This model is based on observations of the bubbles at low system pressures where the fast bubble growth creates a hydrodynamic resistance that makes the bubble almost hemispherical (van Carey 1992). As proved by direct observations (van Ouwerkerk 1972, Torikai *et al.* 1991) through a transparent heating surface, a dry spot (i.e. the spot of the direct contact between the liquid and the vapor) does exist around the nucleation site while the bubble stays near the heating surface. The origin of this dry spot can be explained as follows. First, it is necessary that the vapor-solid adhesion exists to avert the immediate removal of the bubble from the heater by the lift-off forces. This adhesion only appears when the vapor contacts the solid directly. Second, the strong generation of vapor at the triple contact line around the nucleation site prevents the liquid from covering the nucleation site. As a consequence, the existence of the dry spot under a bubble is necessary during its residence time.

Because of the hemispheric bubble shape, the apparent bubble foot is much larger than the dry spot at low heat fluxes. This is why the microlayer model works well at low pressures. For high system pressure, comparable to the critical pressure, the picture is different. The bubble growth is much slower so that the hydrodynamic forces are small with respect to the surface tension. Consequently, the bubble resembles a sphere much more than a hemisphere (van Carey 1992). It is very difficult to identify the microlayer as a thin film in this case.

Nothing definite is known about the microlayer behavior at high heat fluxes close to the CHF. The microlayer dryout models of the CHF have a large degree of uncertainty because they use the parameters of the microlayer calculated to fit the low heat flux data on bubble growth rate. In addition, it is not clear from the physical viewpoint how the part of heater between the bubbles becomes covered by vapor while the heater is completely wetted by the liquid and should therefore always be covered by a liquid film. Because of the small size of the microlayer region, its direct experimental study is very difficult. Rigorous numerical modeling of the microlayer heat transfer is unknown to us. We recently suggested a new approach (Nikolayev and Beysens 1999) to the boiling crisis problem. Based on the concept of the vapor recoil force that we discuss in the next section, it is justified by a rigorous calculation (Nikolayev *et al.* 2001) of the heat transfer near the triple vapor-liquid-solid contact line.

2 Force of vapor recoil and growth of the dry spot under a bubble

Pavlov and Lipchak (1992), Avksentyuk and Ovchinnikov (1995), and Sefiane *et al.* (1998) proposed the vapor recoil instability (Palmer 1976) as a reason for the boiling crisis. Although it is not clear how an instability can induce the spreading of a dry spot, these authors show that the vapor recoil force can be important at large evaporation rates.

Let us introduce the vapor recoil force concept. We consider a portion of the liquid-vapor interface with area A (Fig. 1). The liquid is heated and is thus evaporating. During

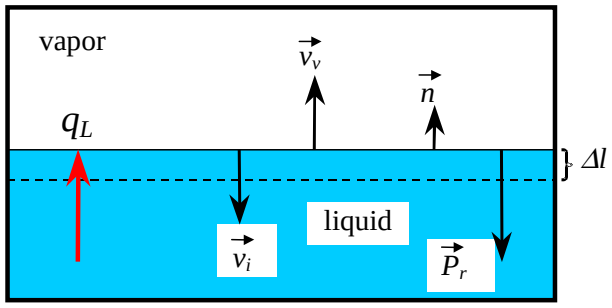

Figure 1: Sketch for the calculation of the expression for the recoil pressure.

the time Δt, the liquid mass Δm (liquid volume ΔV_L) is evaporated. Consequently, the liquid-vapor interface displacement is $\vec{\Delta l} = -\vec{n}\Delta V_L/A$, where $\vec{n}$ is a unit vector normal to the interface directed toward the vapor (Fig. 1). The evaporation also produces a vapor volume ΔV_V. According to mass conservation,

$$\Delta m = \Delta V_L \rho_L = \Delta V_V \rho_V, \tag{1}$$

where ρ_L and ρ_V are the mass densities of the liquid and the vapor. Momentum conservation for this portion of the liquid-vapor interface can be written in the form

$$\Delta m(\vec{v_v} + \vec{v_i}) + \vec{P}_r \Delta t A = 0 \tag{2}$$

where $\vec{P}_r$ is the vapor recoil force per unit area of the interface (i.e., a recoil pressure), $\vec{v_i} = \vec{\Delta l}/\Delta t$ is the interface velocity, and $\vec{v_v} = \vec{n}\Delta V_V/(A\Delta t)$ is the vapor velocity with respect to the interface. Making use of (1), Eq. 2 can be rewritten in the form

$$\vec{P}_r = -\eta^2(\rho_V^{-1} - \rho_L^{-1})\vec{n}, \tag{3}$$

where the rate of evaporation $\eta = \Delta m/(A\Delta t)$ is introduced. It can also be related to the local heat flux q_L per unit area across the interface by the equality

$$q_L = H\eta, \tag{4}$$

where H is the latent heat of evaporation.

Let us now consider a growing vapor bubble attached to the heater surface (Fig. 2). While the temperature of the vapor-liquid interface is constant (in fact, it is the saturation temperature for the given system pressure), a strong temperature gradient forms near the heating surface. The liquid is overheated in a thermal boundary layer of thickness l_r. This

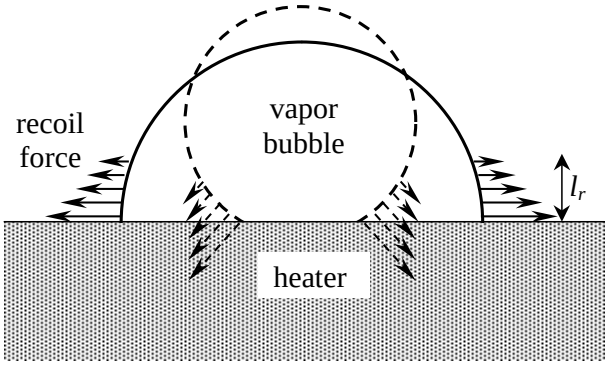

Figure 2: Spreading of the vapor bubble under the action of the vapor recoil force. The thickness l_r of the belt on the bubble surface, in which the vapor recoil force is important, is exaggerated with respect to the bubble radius.

means that the flux q_L is elevated in a "belt" of the bubble surface adjacent to the bubble foot. As a matter of fact, most of the evaporation into the vapor bubble is produced in this belt, whose thickness l_r is usually much smaller than the bubble radius (van Carey 1992). As follows from (3, 4), the vapor recoil near the contact line is much larger than on the other part of the bubble surface. Consequently, the bubble should deform as if the triple contact line were pulled apart from the bubble center as shown in Fig. 2. This means that under the action of the vapor recoil the dry spot under the vapor bubble should spread covering the heater surface.

In the following subsection, we will show in a simple example that the influence of the vapor recoil can be interpreted in terms of a change of an apparent contact angle.

2.1 Vapor recoil and apparent contact angle.

Let us consider a curvilinear coordinate l measured along the bubble contour, which is perpendicular to the heater plane, as it is shown in Fig. 3. By apparent contact angle

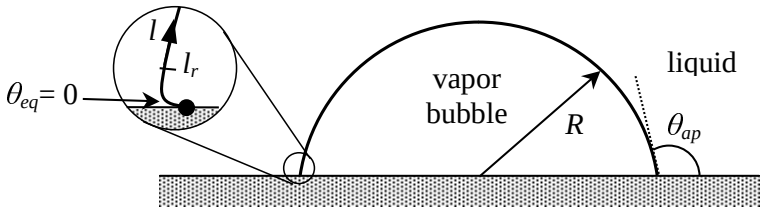

Figure 3: The apparent contact angle θ_{ap} and the actual contact angle θ_{eq}. While the apparent contact angle is large, the insert shows that the actual contact angle is zero. The black point denotes the intersection of the bubble contour with the contact line, i.e. zero for the curvilinear coordinate l.

θ_{ap}, we mean the angle between the tangent to this bubble contour and the heater plane measured at $l = l_r$, where l_r was defined in the previous section. Since $l_r \ll R$, θ_{ap} seems to be the actual contact angle to an observer that cannot see the details much smaller than the length-scale R. However, zooming in to the scale l_r would reveal the actual contact angle that can differ strongly from θ_{ap} as it is shown in the insert of Fig. 3. In

the following, we assume that the motion of the contact line is slow enough so that the actual contact angle is given by its equilibrium value θ_{eq}.

Suppose that l_r is so small that the function $P_r(l)$ can be approximated by the Dirac δ-function:

$$P_r(l) = \sigma_r \delta(l). \tag{5}$$

This means that the vapor recoil is localized at the contact line. This example may seem nonphysical because $P_r(0) \to \infty$. However, a rigorous calculation (Nikolayev and Beysens 1999) shows that P_r can diverge provided that the integral of $P_r(l)$ is finite. Eq. 5 satisfies this condition because the integral of the δ-function is equal to unity.

Note that the amplitude of the vapor recoil σ_r has the dimension of a surface tension and can thus be included in the Young balance of the tensions acting on the contact line (Fig. 4). The contact line is stationary when the horizontal component of the vector sum

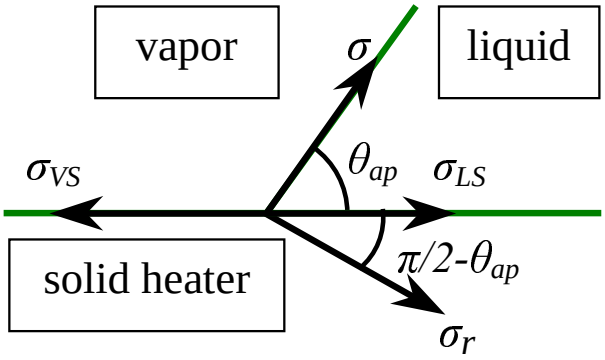

Figure 4: Balance of the forces that act on the triple contact line, where σ, σ_{VS} and σ_{LS} are the surface tensions for vapor-liquid, vapor-solid and liquid-solid interfaces respectively.

of all the forces is equal to zero. It can be shown from Fig. 4 that this condition is

$$\cos\theta_{ap} = \cos\theta_{eq} - N_r \sin\theta_{ap}, \tag{6}$$

where the equilibrium contact angle is given by the expression $\cos\theta_{eq} = (\sigma_{VS} - \sigma_{LS})/\sigma$. The parameter

$$N_r = \frac{\sigma_r}{\sigma} = \frac{1}{\sigma} \int_0^{l_r} P_r(l)\,\mathrm{d}l \tag{7}$$

characterizes the strength of the vapor recoil relative to the vapor-liquid surface tension σ. The expression (6) can also be obtained by using a more rigorous approach (Nikolayev and Beysens 1999).

The dependence of θ_{ap} on N_r calculated from (6) is presented in Fig. 5. It can be seen that the vapor recoil force increases the apparent contact angle. When the power of the heater is kept constant, the heat flux q_L increases with time, usually by following a square root law. Consequently, P_r and N_r grow with time in accordance with (3, 4, 7). Therefore, the apparent contact angle should grow with time as is sketched in Fig. 2. This increase leads to the spreading of the dry spot. The dry spot always remains of finite size (which fits the experimental results of van Ouwerkerk (1972) and Torikai *et al.* (1991)) because, according to Fig. 5, $\theta_{ap} < \pi$ even for a large N_r.

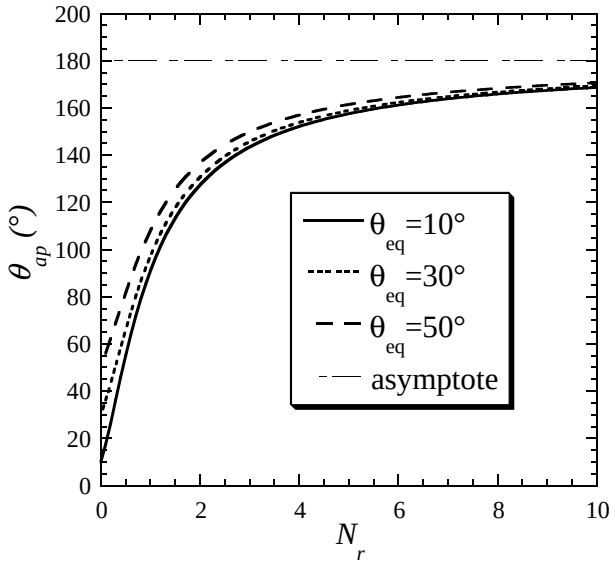

Figure 5: Apparent contact angle versus the strength of the vapor recoil N_r for the different values of the equilibrium contact angle.

2.2 Numerical simulation of the bubble growth

In reality, the vapor recoil is not localized *exactly* on the contact line as it was assumed in the approximation (5) treated in the previous subsection. We present here the more general results of a numerical simulation of a growing vapor bubble. Since we do not use any assumptions about the shape of a "microlayer" or of the heat transfer in it, we expect to obtain a realistic picture. The calculation of the heat transfer around a growing vapor bubble is a free boundary problem that is quite difficult. We therefore need to accept several simplifying assumptions. We assume a very slow growth, corresponding to the regime of high system pressure, so that we can neglect the liquid motion that appears from the interface motion and from thermal convection. In this case, the bubble shape is defined only by the forces of surface tension and vapor recoil. The shape can be calculated from the equation (Nikolayev and Beysens 1999)

$$K\sigma = \lambda + P_r, \tag{8}$$

where K is the local curvature of the bubble and λ is a constant Lagrangian multiplier (the difference in pressures outside and inside the bubble) to be determined by using the given volume V of the bubble. Note that Eq. 8 is a 2nd order differential equation for a function that defines the bubble contour. Its first derivative on the contact line is related to the value of the actual contact angle that is chosen to be zero for the present simulation. This relation serves as a boundary condition so that the bubble shape can be determined from (8) at each time step.

The statement of the transient thermal conduction problem in liquid is conventional for the thermally controlled bubble growth under the conditions of the saturated boiling (Tong 1997) except for a boundary condition on the surface of the heater. We cannot impose either the uniform heat flux or the uniform temperature boundary condition on the heater. This is because of the unphysical divergence of the heat flux through the bubble interface that would appear in the vicinity of the triple (vapor-liquid-heater) contact line in both of these cases resulting in a large error in the dry spot size. The uniform temperature

boundary condition generates an unphysical divergence because of the following ambiguity. On one hand, the temperature of the triple contact line should be above the saturation temperature since this line is on the heater that supplies the energy. On the other hand, the temperature of the triple contact line should be equal to the saturation temperature since this line also belongs to the bubble interface. The uniform heat flux boundary condition is unsuitable because the heat flux through the dry spot under the bubbles ought to be nearly zero (because the vapor is a bad heat conductor) while the heat flux should be much larger on the other part of the heater. Therefore, the transient thermal conduction problem inside the heater needs to be considered.

We assume that the known heat power $j(t)$ is generated uniformly inside the heater. The heat flux from the heater to the fluid $q_s = q_s(x,t)$ is the most important control parameter. Its value at a point far from the bubble $q_s|_{x\to\infty}$ depends only on the particular choice for the function $j(t)$. For simplicity, we choose $j(t) \propto t^{-1/2}$ because the flux at infinity $q_0 = q_s|_{x\to\infty}$ turns out to be time-independent in this case.

We assume that a circular bubble has already nucleated at the heater surface at $t = 0$ with no initial superheating. The initial superheating would accelerate the bubble growth slightly at the initial stages. This acceleration would not be important for the dry spot spreading that becomes significant later on.

The above problem has been solved by the Boundary Element Method in 2D for the values of the numerical parameters that correspond to water at 10 MPa in contact with the stainless steel heater. The simulation is discussed in detail by Nikolayev *et al.* (2001). We would like to present here only the main results.

The time evolution of the bubble shape is shown in Figs. 6. At low heat flux, the

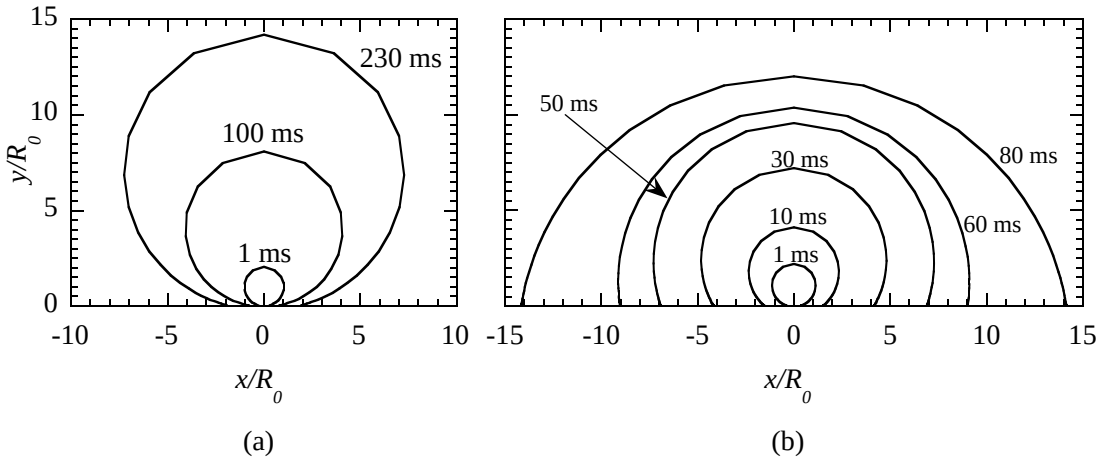

Figure 6: The bubble shape shown for different growth times. The heat fluxes from the heater are a) $q_0 = 0.05$ MW/m^2; b) $q_0 = 0.5$ MW/m^2. The coordinates are scaled by the initial bubble radius R_0.

shape of the bubble stays nearly spherical (Fig. 6) during the calculation time. Fig. 6b shows that at large heat flux the radius of the dry spot can exceed the bubble height, thus confirming the previous theoretical predictions (cf. Fig. 2). It is easy to see that the apparent contact angle grows with time, although the *actual* contact angle remains zero during the evolution. The large apparent contact angle is due to the strong change in slope of the bubble contour near the contact line.

The temporal evolution of the radius R_d of the dry spot is illustrated in Fig. 7, where the time evolution of R_d/R is shown. R is the drop radius defined as the maximum

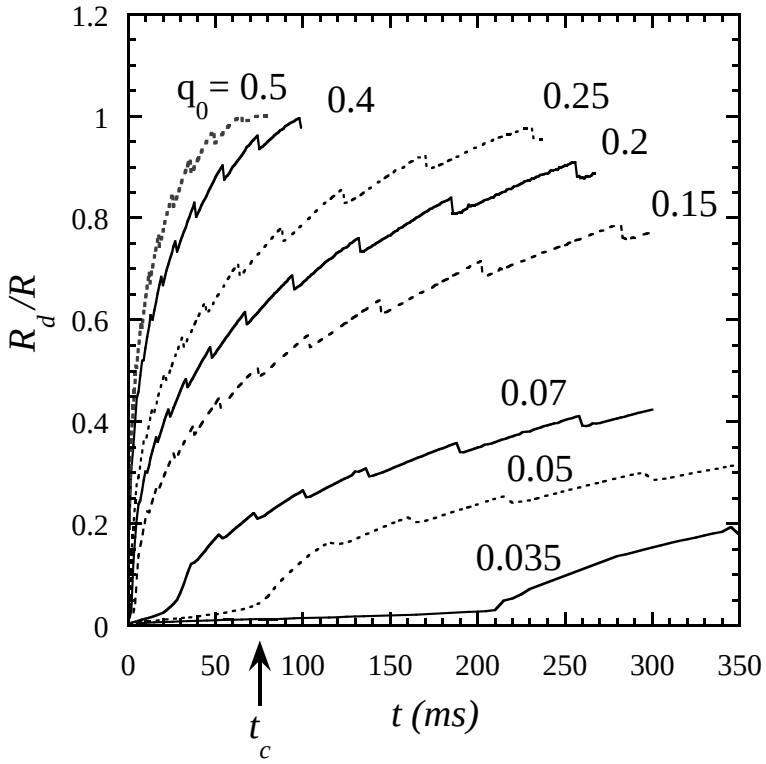

Figure 7: The temporal evolution of the ratio of the dry spot radius R_d and the bubble radius R for different values of the heat flux form the heater q_0 (MW/m^2). The transition time t_c is shown for the curve that corresponds to $q_0 = 0.05$ MW/m^2.

abscissa for the points of the drop contour, so that $R_d/R \leq 1$. One can see that the dry spot remains small until a transition time t_c. At this point the growth of the dry spot accelerates steeply (see Fig. 7). This time t_c corresponds to the moment where the vapor recoil force overcomes the surface tension and the bubble begins to spread. This transition time is an increasing function of q_0. The oscillations of the curves in Fig. 7 are not numerical artifacts. They appear as a result of an instability. Its discussion is out of the scope of the present article.

3 A scenario for boiling crisis

A numerical estimate (Nikolayev and Beysens 1999) shows that the vapor recoil overcomes the surface tension when the heat flux q_0 is of order of the experimentally found values for q_{CHF}. Since the vapor recoil is time-dependent, we need to consider the characteristic times of this problem. The first of them is t_c, it is when the bubble spreading begins. There is another characteristic time, the bubble residence time t_{dep}, which is the time during which the bubble is attached to the heater. The value of t_{dep} increases with the adhesion force (that keeps the bubble near the heater) and depends on the external conditions such as flow, presence of gravity, etc. It is evident that the occurrence of the bubble spreading depends on the interrelation between t_c and t_{dep}: the spreading is

possible when $t_c < t_{dep}$. However, the spreading influences t_{dep} itself because the bubble adhesion force is proportional to the contact line length (van Helden *et al.* 1995) which increases with the dry spot size. Clearly, t_c is a decreasing function of q_0 (see Fig. 7). This means that, while the bubble spreading should not occur when q_0 is even slightly less than some threshold value, the bubble spreading will continue once it begins (bubbles will grow while attached to the heater by the increasing adhesion) at or above the threshold. We associate this threshold for q_0 with the CHF.

Without the calculation of the residence time, it is not possible to determine a precise value for q_{CHF}. However, we can use the above considerations to explain qualitatively the experimentally observed tendencies.

The residence time measured even far from the boiling crisis can give important information about the CHF itself. When t_{dep} is large because of the external conditions (as under reduced gravity conditions or when the fluid is heated from above), the CHF should be small because the dry spot has enough time to achieve a sufficiently large size at smaller q_0. Similarly, the decrease of t_{dep} with an increasing flow velocity for flow boiling should increase the CHF (the fluid flow facilitates the bubble departure). The experimental data confirm this conjecture of our model, see e.g. Brusstar and Merte (1998). Brusstar *et al.* (1999) came to the same conclusion after having analyzed their experimental results on flow boiling. They found $q_{CHF} \propto t_{dep}^{-1}$.

The strong dependence of the CHF on the equilibrium contact angle, that was observed by Diesselhorst *et al.* (1981) is a natural consequence of the present model. The dry spot is larger initially for the larger contact angle. A smaller heat flux is thus needed to achieve the spreading of the bubble illustrated by Figs. 2 and 6b.

4 Experimental evidence of the bubble spreading

The experiments carried out by our group (see Garrabos *et al.* 1999) confirm that our model of the bubble spreading is valid in the near-critical region, i.e. for the system pressure and temperature that are close to the critical pressure and temperature for the given fluid. The critical point exhibits many singular properties. In particular, the coefficient of thermal diffusion vanishes. The bubble growth thus slows down in the near-critical region. In fact, we could observe the growth of a single bubble during about fifteen minutes.

Since the surface tension also vanishes at the critical point, the vapor bubbles of the usual convex shape are not observable under Earth's gravity. For this reason our experiment was performed onboard the Mir space station. The CHF value vanishes at the critical point. Therefore, even a very slow heating rate is expected to produce bubble spreading. Because of the slow evolution, the hydrodynamic effects are very small and the bubble shape is not distorted by them according to what was assumed for our theoretical modeling. A cylindrical experimental cell was filled by SF_6 at nearly critical density, see Garrabos *et al.* (1999) for details. The bubble evolution was observed through the transparent bases of the cylindrical cell. The equilibrium value of the contact angle is zero so that the initial bubble shape is nearly circular. The bubble is shifted to the side of the cell because the windows of the cell are slightly inclined with respect to each other.

While the radius of the cell is 6 mm, its height is only 1.66 mm. Such a constrained bubble has a large portion of its interface separated from the heating surface by a thin

wetting film. This liquid film plays a role of the microlayer that is quickly evaporated thus forming a dry spot that favors its further spreading. The temporal evolution of the bubble is shown in Fig. 8. The apparent contact angle clearly increases with time.

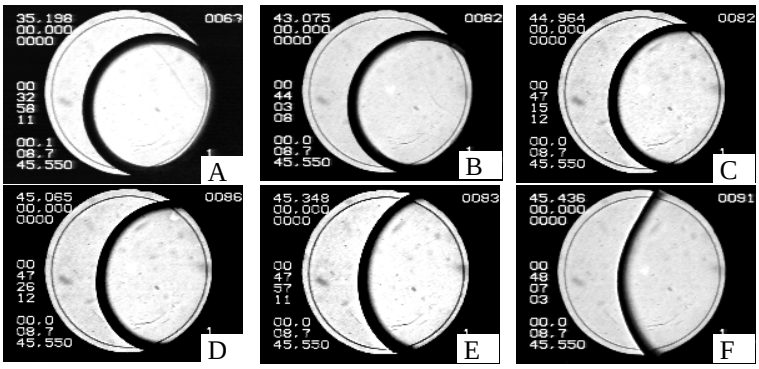

Figure 8: Temporal sequence of images of a vapor bubble in a cylindrical cell in near-critical SF_6. The images were obtained during continuous heating of the cell. The last image (F) corresponds to the temperature just below the critical temperature. The increase of the apparent contact angle is obvious.

Although the volume of the vapor bubble does not change, the vapor mass grows due to the growing mass density. Unlike the low-pressure regime, the density depends strongly on temperature in the near-critical region.

5 Conclusions

We propose a physical explanation for the boiling crisis based on the growth of the dry spot under a vapor bubble caused by the vapor recoil force. The theoretical approach is supported by the numerical simulation of the bubble growth at a large heat flux and by the experimental data on growth of the vapor bubble in near critical fluid performed under microgravity conditions. The proposed criterion for the boiling crisis provides a physical basis for further studies. It explains qualitatively the dependence of the critical heat flux on some key physical parameters.

References

Avksentyuk B. P. & Ovchinnikov V. V. (1995) Burnout model for pool and forced flow boiling. In *Two-Phase Flow Modelling and Experimentation*, Eds. G. P. Celata & R. K. Shah, Edizioni ETS, 1205–1210.

Bricard P., Péturaud P. & Delhaye J.-M. (1997) Understanding and modeling DNB in forced convective boiling: Modeling of a mechanism based on nucleation site dryout. *Multiphase Sci. Techn.* **9**, No. 4, 329–379.

Brusstar M. J., Merte H., Keller R. B. & Kirby B. J. (1997) Effects of heater surface orientation on the critical heat flux — I. An experimental evaluation of models for subcooled pool boiling. *Int. J. Heat Mass Transfer* **40**, 4007–4019.

Brusstar M. J. & Merte H. (1998) An experimental and theoretical approach to modeling the CHF for forced convection in microgravity. In *Proc. of 11th Int. Heat Transfer Conf.*,

Kyongju (S.Korea), Vol. 2, 231–236.

Buyevich Yu. A. (1999) Towards a Unified Theory of Pool Boiling — the Case of Ideally Smooth Heated Wall. *Int. J. Fluid Mech. Res.*, **26**, 189–223.

van Carey P. (1992) Liquid-Vapor Phase Change Phenomena. Hemisphere, Washington D.C.

Cooper M. G. & Lloyd A. J. P. (1969) The microlayer in nucleate pool boiling. *Int. J. Heat Mass Transfer* **12**, 895–913.

Diesselhorst T., Grigull U. & Hahne E. (1977) Hydrodynamic and surface effects on the peak heat flux in pool boiling. In *Heat Transfer in Boiling*, Eds. E. Hahne & U. Grigull, Hemisphere, 99–135.

Garrabos Y., Chabot C., Wunenburger R., Delville J.-P., & Beysens D. (1999) Critical boiling phenomena observed in microgravity. *J. Chimie Physique* **96**, 1066–1073 .

van Helden W. G. J. , van der Geld C. W. M. & Boot P. G. M. (1995) Forces on bubbles growing and detaching in flow along a vertical wall. *Int. J. Heat Mass Transfer* **38**, 2075–2088.

Kenning D. B. R. & Del Valle M. V. H. (1981) Fully-developed nucleate boiling: overlap of areas of influence and interference between bubble sites. *Int. J. Heat Mass Transfer* **24**, 1025–1032.

Nikolayev V. S. & Beysens D. A. (1999) Boiling crisis and non-equilibrium drying transition. *Europhysics Letters* **47**, 345–351.

Nikolayev V. S., Beysens D. A., Lagier G.-L., & Hegseth J. (2001) Growth of a dry spot under a vapor bubble at high heat flux and high pressure. *Int. J. Heat Mass Transfer*, **44**, 3499–3511.

van Ouwerkerk H. J. (1972) Burnout in pool boiling: the stability of boiling mechanisms. *Int. J. Heat Mass Transfer* **15**, 25–34.

Palmer H. J. (1976) The hydrodynamic stability of rapidly evaporating liquids at reduced pressure. *J. Fluid. Mech.* **75**, part 3, 487–511.

Pasamehmetoglu K. O. & Nelson R. A. (1991) Cavity-to-cavity interaction in nucleate boiling: the effect of heat conduction within the heater. *AIChE Symp. Ser.* **87** No. 283, 342–351.

Pavlov P. A. & Lipchak A. I. (1992) About the non-hydrodynamic causes of the boiling crisis. In *Metastable Phase States and Kinetics of Relaxation*, Russian Acad. Sci., Ural Division, Sverdlovsk, 119–125 (in Russian).

Sefiane K., Benielli D. & Steinchen A. (1998) A new model for pool boiling crisis, recoil instability and contact angle influence. *Colloids and Surfaces* **142**, 361–373.

Tong L. S. (1997) Boiling Heat Transfer and Two-Phase Flow (2nd Edn.), Taylor & Francis, New York.

Torikai K., Suzuki K. & Yamaguchi M. (1991) Study on Contact Area of Pool Boiling Bubbles on a Heating Surface (Observation of Bubbles in Transition Boiling). *JSME Int. J. Series II* **34**, 195–199.

Yiantsios S. G. & Davis R. H. (1991) Close approach and deformation of two viscous drops due to gravity and van der Waals forces. *J. Colloid Interface Sci.* **144** 412–433.